Annales Geophysicae

Climatic trends in E-region critical frequency and virtual height above Tromsø (70° N, 10° E)

C. M. Hall[1], A. Brekke[2], and P. S. Cannon[3]

[1]Tromsø Geophysical Observatory, University of Tromsø, Norway
[2]Dept. of Physics and Technology, University of Tromsø, Norway
[3]Qinetiq, Malvern, UK

Abstract. We have examined the long time series of observations of E-region virtual height (1948–2006) and critical frequency (1935-2006) hitherto made by the Tromsø ionosonde at 70° N, 19° E. Combining a simplistic trend analysis with a rigorous treatment of errors we identify a negative trend in critical frequency. While a similar analysis of the virtual height $h'E$ also suggests a negative trend, a closer examination reveals a possible weak positive trend prior to $\sim$1975 and a strong negative trend from $\sim$1975 to present. These two metrics of essentially the same feature of the ionosphere do not exhibit the same signature since critical frequency is controlled by photochemistry within the E-layer while height is controlled by pressure level. We further find that the trend in critical frequency is a daylight/summer phenomenon, no significant trend being evident in the winter subset of the data. On the other hand, the trends in virtual height are independent of season/daylight.

Keywords. Ionosphere (Auroral ionosphere; Ionosphere-atmosphere interactions)

1 Introduction

In this study on long term changes in the E-region ionosphere, we try to differentiate between solar and terrestrial induced changes, although this is somewhat artificial, since the Earth's climate is inexorably governed by the sun. An often-used approach is to subtract the effects of solar radiation from a geophysical time series such that the residual indicates climatic change originating from the biosphere or long term changes due to other causes, such as the solid earth. At best ionospheric studies have 70 years of data to work with, of which only 20–30 years (i.e. only 2 solar cycles)

Correspondence to: C. M. Hall
(chris.hall@tgo.uit.no)

might be expected to be grossly affected by, for example, pollution from jet engines.

Many searches for climatic change in the mesosphere and thermosphere have been performed, in particular during the last two decades. Roble and Dickinson (1989) for example have modelled the influence of greenhouse gas (in particular CO_2 and CH_4) variability on the temperature and density structures of the mesosphere and thermosphere and Rishbeth (1990) has used these findings to examine the ionospheric response. Measurements of ionospheric parameters, largely by ionosondes, have been examined for a number of geographical locations with a view to attributing trends to anthropogenic sources (to give a few examples: Ulich and Turunen, 1997; Bremer, 1998 and 2001; Jarvis et al., 1998; Hall and Cannon, 2001 and 2002; Cannon et al., 2004; Qian et al., 2006). These studies have addressed trends in F-and E-region critical frequencies and virtual heights, and while little doubt remains that local changes are occurring at some locations, the underlying local and global mechanisms remain unclear.

A common factor in these studies is the removal of extraterrestrial forcing. This is usually achieved by performing a regression between the ionospheric parameter in question and, for example, sunspot number, the f10.7 flux, and/or a geomagnetic index. Removal of the direct solar influence effectively filters out the solar cycle dependence and a suitable geomagnetic index reflects the solar modulated variation in ionospheric current systems. The start date of the ionospheric time series in question dictates which solar parameters can be used.

A series of ionosondes have been in operation at Tromsø since 1935 (Hall and Hansen, 2003) but initially only critical frequencies were measured and these only at selected times during the working day. The determination of virtual heights began in 1948. For studies such as reported here, it is important to be aware of changes in location and configuration as these could affect trend analyses; in the results that follow

Fig. 1. Monthly medians of mid-day values of foE (upper panel) and $h'E$ (lower panel).

Fig. 2. Scatter plots of foE (upper panel) and $h'E$ (lower panel) versus sunspot number (SNN). Solid red lines show the minimized absolute deviation linear fits, red dashed lines the extremes derived from standard deviations in gradients and intercepts of the fit, and the orange lines show the extents of the mean standard deviation of the individual absolute deviations. There is a 15% uncertainty in the gradient of the linear regression of foE on SNN and a 23% uncertainty for $h'E$.

we have indicated dates of these major changes. In order to maximize use of the time series we have used only the 10:00 UT (or 12:00 LT in early years) soundings, a philosophy which minimizes data-gaps because historically there was almost always a mid-day sounding. Owing to the high latitude of the station, this also has the effect of providing a low solar elevation series by selecting winter data and a high solar elevation series by selecting non-winter data, as Hall and Cannon (2002) did in order to demonstrate the darkness-daylight difference in F-region trends.

In this study, our focus is on the E-region which is well described by a simple Chapman layer, rather than the more complicated combination of dynamics and ion chemistry found in the F-region above. Furthermore, since there is normally little ionosphere underlying the E-region, the virtual heights, $h'E$, are more likely to represent the true layer heights than in the F-region case.

2 Results

Trend analyses have been performed with a variety of conditioning of the data and careful treatment of errors and their propagation (Taylor, 1997). Fig. 1 shows the monthly medians of daily mid-day E-region critical frequencies (foE) and the monthly medians of daily mid-day virtual heights ($h'E$) that represent the starting point for this study. Here we see clearly the seasonal variations and also the quasi 11 year solar cycle variation, the latter particularly in foE. One can also discern trends in foE and in the latter two decades of
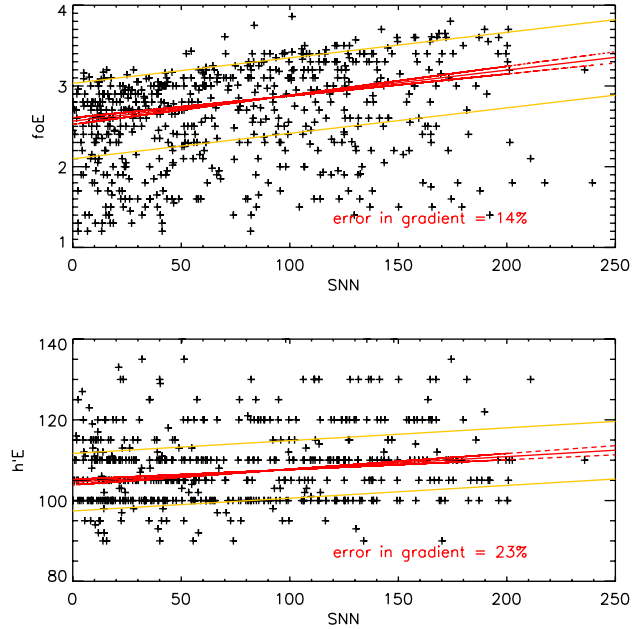
$h'E$. Another feature of interest is the changing measurement precision of $h'E$ partly made visible by our use of medians rather than means – resolution better than 5 km was essentially never attempted in early years of observation. In Fig. 2 we show scatter plots of the data from Fig. 1 versus monthly sunspot number (SNN) (information from the Space Environment Center, Boulder, CO, National Oceanic and Atmospheric Administration (NOAA), U.S. Dept. of Commerce). With frequencies in MHz and heights in km:

$$foE' = foE - (2.6 + 0.003\text{SNN}) \qquad (1)$$

$$h'E' = h'E - (105 + 0.03\text{SNN}) \qquad (2)$$

wherein the uncertainty in the dependence of foE on SNN is 15% and that of $h'E$ on SNN is 23%. We now follow two lines of approach, one being to look for trends in the residuals foE' and $h'E'$, and the other to simply use foE and $h'E$. The former is the classic method (e.g. Ulich and Turunen, 1997) whereas the latter is very simplistic.

Taking the simplistic approach first, we smooth the foE and $h'E$ timeseries using a 22 year running mean (i.e. 132 point wide boxcar filter) and reject 11 years of data at each end and apply minimum absolute deviation fits. The results are shown in Fig. 3. The mid-day monthly medians are depicted by + symbols, the thick blue lines are the smoothed
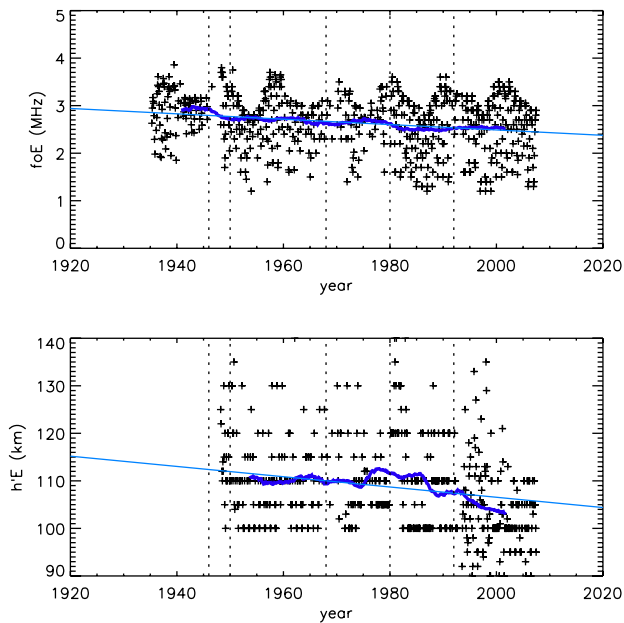
Fig. 3. Trends in foE (upper panel) and $h'E$ (lower panel). Individual symbols show the monthly mid-day medians (as in Fig. 1.); thick blue lines: smoothed time series; thin blue lines: linear fits to smoothed data; vertical dotted lines indicate dates when system changes were made. The trends are as follows: foE, -0.06 MHz decade$^{-1}\pm1\%$; $h'E$, -1.1 km decade$^{-1}\pm3\%$.

Fig. 4. Trends in foE' (upper panel) and $h'E'$ (lower panel). Individual symbols show the monthly mid-day medians (as in Fig. 1.); thick green lines: smoothed time series; thin blue lines: ±1-sigma limits to the linear fits to the smoothed data obtained from the mean standard deviation of the individual absolute deviations in the linear fits shown in Fig. 2; vertical dotted lines indicate dates when system changes were made. The trends are as follows: foE', -0.05 MHz decade$^{-1}\pm2\%$; $h'E'$, -1.0 km decade$^{-1}\pm6\%$.

time series described above and the thin blue lines are the fits to the smoothed data. Dates on which changes to the radar system were performed are indicated by vertical dashed lines. There are no obvious discontinuities in the frequency data corresponding to any of the system changes, however, better height resolution resulted from the introduction of the current digital system in 1992. The trend in foE is found to be -0.06 MHz decade^{-1} with an uncertainty of $\pm1\%$, and that in $h'E$ to be -1 km decade$^{-1}\pm3\%$. Repeating the process using the residuals foE' and $h'E'$ (Fig. 4) we obtain a trend in foE' of -0.05 MHz decade$^{-1}\pm2\%$ and in $h'E'$ of -1 km decade$^{-1}\pm6\%$. In the figure the green lines indicate the smoothed data while the blue lines indicate the ±1-sigma spread in the trends corresponding to the mean standard deviation of the individual absolute deviations in the linear fits of the time series to the SNN. The 22 year period ripple remaining in the foE' data is within ±2-sigma, and similarly for the remaining variability in $h'E'$.

The smoothed foE and foE' values and their respective trend lines strongly suggest a steady decrease in electron density with time. On the other hand, the corresponding plots for $h'E$ and $h'E'$ indicate fairly constant values until the late 1970's and a negative trend only during the last 3 decades. We have, therefore, divided the $h'E'$ time series into two: pre-1980 and post-1980. The choice of 1980 is somewhat arbitrary, and is the approximate midpoint. We then fit
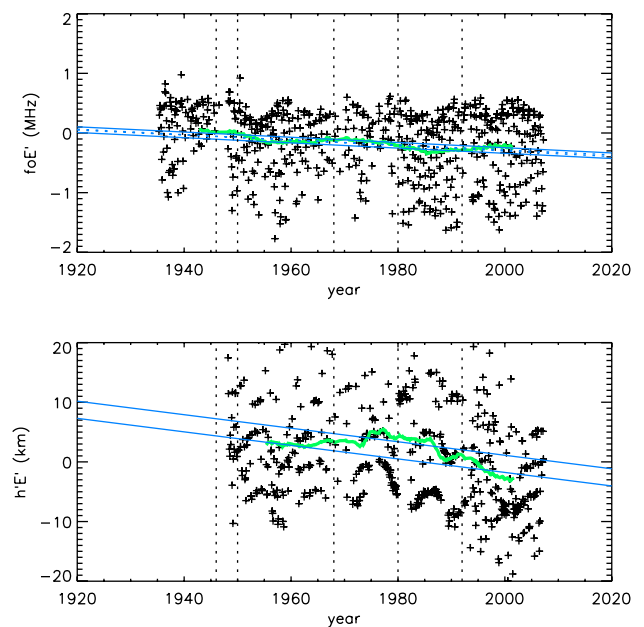
trend-lines to both frequency and height, and this time use a minimum chi-squared error statistic method which enables us to take account of the uncertainty in the data points that has propagated from the subtraction of the SNN dependent component (as was shown in Fig. 2). This slightly different method incorporating a more rigorous propagation of errors also yields a trend of -0.05 MHz decade^{-1} for foE', with a more conservative uncertainty of 25%. (Fig. 5) but essentially reproducing the earlier result. For the split time series of $h'E'$ we obtain a positive trend prior to 1980 of 0.7 km decade$^{-1}\pm92\%$ and a negative trend after 1980 of -3.8 km decade$^{-1}\pm19\%$ (also Fig. 5). There is considerable uncertainty in the pre-1980 result; selection of other subsets of the time series fail to yield conclusive evidence for either significant positive or negative trends in the early half. On the other hand a decrease in altitude of the E-region in the last 2–3 decades seems incontestable.

3 Discussion

The E-region virtual height and its critical frequency do not exhibit the same signatures in trend: while the former is controlled by pressure levels connected to thermal changes in the *underlying* atmosphere, the latter is controlled by
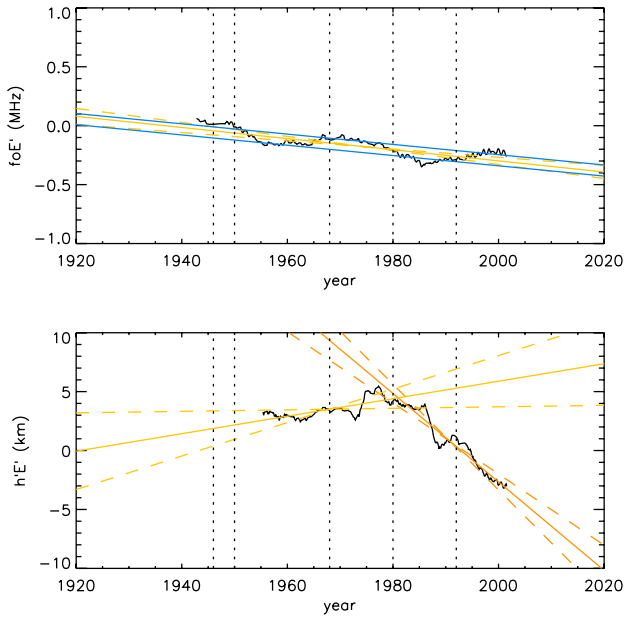
Fig. 5. Trends in foE' (upper panel) and $h'E'$ (lower panel) using the minimum chi-squared method and dividing the $h'E'$ time series into pre and post 1980 parts. Black lines: smoothed time series; solid lines show the linear fits, dashed lines the uncertainties; vertical dotted lines indicate dates when system changes were made. For fits to $h'E'$, light orange is used for the pre-1980 subset and dark orange for the post-1980 subset. The trends are as follows: foE', -0.05 MHz decade$^{-1}\pm25\%$; $h'E$ pre-1980, $+0.7$ km decade$^{-1}\pm92\%$; $h'E$ post-1980, -3.8 km decade$^{-1}\pm19\%$.

photochemistry *within* the layer. Similarly, there are essentially two scenarios for climate change in the upper atmosphere caused by increasing CO_2 and CH_4. In one, increasing concentrations of greenhouse gases lead to increasing radiative cooling and, therefore, a shrinking of the middle atmosphere, and thereafter the overlying ionosphere forming progressively lower down. In this situation, the electron densities of the ionospheric layers remain unchanged: the peaks occur at the same pressure surfaces, but the latter are simply lowered as the underlying atmosphere occupies less volume. In the second scenario the greenhouse gases affect the ionospheric layers in situ. It is reasonable to assume that both processes actually occur because the gases themselves will first affect the middle atmosphere and then continue to diffuse upwards possibly undergoing chemical change, to eventually affect the composition of the lower thermosphere.

The evidence presented hitherto indicates that there has been (presumably still is) a lowering of the E-region since the late 1970's, but before that it is impossible to identify any trend with any degree of certainty. On the other hand, the E-region electron density has been steadily decreasing since 1935, a phenomenon not consistent with a simple lowering of the ionosphere.

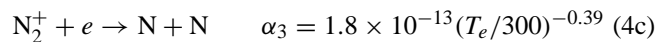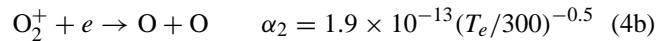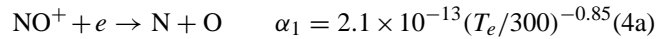The electron production rate at the E-region maximum,

Table 1. How electron density depends on temperature, T^n for different primary positive ion species and day and night conditions.

Species	n (day)	n (night)
O_2^+	$(-1+0.5)/2=-0.25$	$0.5/2=+0.25$
NO^+	$(-1+0.85)2=-0.08$	$0.85/2=0.43$

q_m, is inversely proportional to the scale height, H, and, therefore, also inversely proportional to the neutral temperature T:

$$q_m = \frac{C \cdot I_\infty}{e \cdot H} \cos\chi \tag{3}$$

where C is the ionisation efficiency, I_∞ is the solar radiation intensity prior to absorption by the atmosphere, and χ is the solar zenith angle. C is unity for atomic species since all of the energy goes into producing ion-electron pairs, but is less than unity for ionisation of molecules. The electron loss is primarily by dissociative recombination with rates α_1, α_2 and α_3 corresponding to the dominant E-region ion species:

$$NO^+ + e \rightarrow N + O \qquad \alpha_1 = 2.1 \times 10^{-13}(T_e/300)^{-0.85} \tag{4a}$$

$$O_2^+ + e \rightarrow O + O \qquad \alpha_2 = 1.9 \times 10^{-13}(T_e/300)^{-0.5} \tag{4b}$$

$$N_2^+ + e \rightarrow N + N \qquad \alpha_3 = 1.8 \times 10^{-13}(T_e/300)^{-0.39} \tag{4c}$$

The net recombination rate α is thus approximately inversely proportional to the square root of the electron temperature, T_e. In the collision dominated E-region, T_e can be assumed to be very similar to T, on average. The peak electron number density is given by

$$n_e = \sqrt{q_m/\alpha} \tag{5}$$

and thus during daylight hours the electron density at the E-region peak depends roughly on $T^{-0.25}$ (Brekke, 1997; Hargreaves, 1992). From Eqs. (3), (4a–c) and (5) we find the temperature dependencies summarized in Table 1. We have, therefore, performed separate trend analyses for "daylight" and "darkness" data. Since all data are from 12:00 LT (early in the time series) or 10:00 UT (later in time series) and since Tromsø is a high latitude station, we achieve this by selecting summer data corresponding to daylight conditions and winter data approximating to darkness. For critical frequency analyses we use June and December values respectively, while for virtual height we use {May, June, July} and {November, December, January} respectively since data are more sparse. These data and their trends and uncertainties are shown in Figs. 6 and 7. Immediately apparent from Fig. 6 is that the negative trend in foE' is a daylight/summer phenomenon only which would indicate a warming of the ionosphere and background neutral atmosphere.
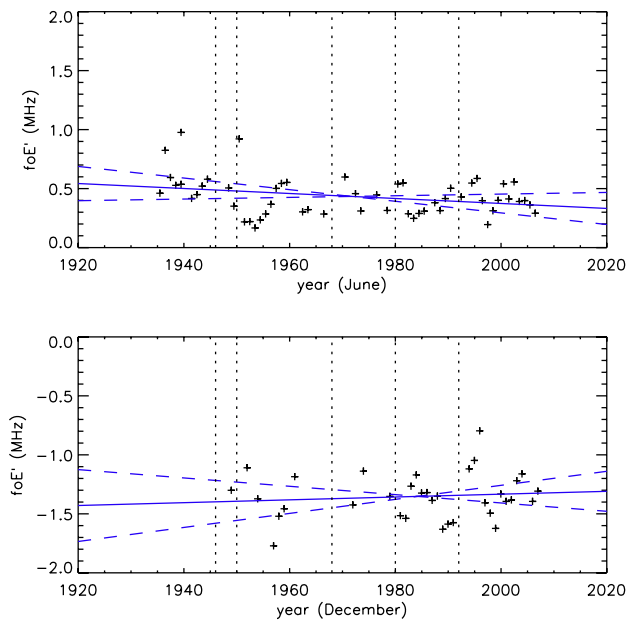
Fig. 6. Values, trends and uncertainties in foE' from June (upper panel) and December (lower panel). The trends are as follows: June, -0.02 MHz decade$^{-1}\pm130\%$; December $+0.01$ MHz decade$^{-1}\pm488\%$.
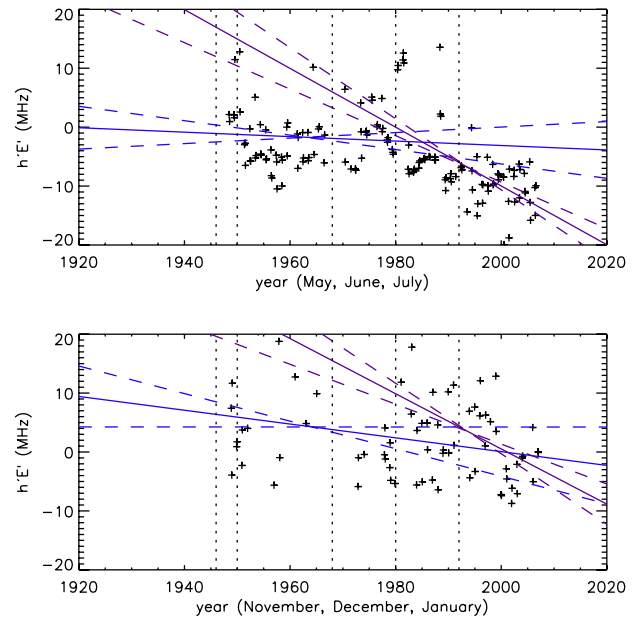

Fig. 7. Values, trends and uncertainties in $h'E'$ from {May, June and July} (upper panel) and {November, December and January} (lower panel). The trends are as follows: summer, pre-1980, -0.4 km decade$^{-1}\pm226\%$; summer, post-1980, -5.0 km decade$^{-1}\pm20\%$; winter, pre-1980, -1.2 km decade$^{-1}\pm100\%$; winter, post-1980, -5.0 km decade$^{-1}\pm27\%$.

For $h'E'$, we find that the post 1980 trends are similar for winter and summer conditions. Prior to 1980, we see weak negative trends, albeit with considerable uncertainty. The negative trend during darkness/winter is significant, the "flatter" of the two 1-sigma uncertainty limits having a zero trend, although still considerably weaker than post 1980. This difference in pre- and post-1980 characteristics suggest that there are different mechanisms for the trends in $h'E'$ before and after ∼1980.

As seen from Table 1, if the dominant positive ion is O_2^+, $n_e\propto T^{-0.25}$ during the day and $n_e\propto T^{0.25}$ at night. A negative trend in foE would therefore be commensurate with in situ cooling if that trend was evident in the night (i.e. approximated here by winter subset of the timeseries) only. If the dominant ion was NO^+, n_e would be approximately independent of temperature during the day (i.e. approximated here by summer subset of the timeseries). Danilov (2001) has discussed this briefly and tentatively associates an increasing foE with decreasing NO^+/O_2^+ ratio, the latter conceivably caused by increasing downward transport of NO by turbulent diffusion. This scenario is supported by observations of increasing D-region electron density (Danilov, 1997) which could be associated with smearing out of the NO minimum at ∼85 km altitude by turbulence, a climatic increase in turbulent intensity above ∼80 km having been reported by Hall et al. (2007). Depletion of NO in the E-region would, however, cause an increase in foE due to reduced dissociative recombination (a decreasing $[NO^+]/[O_2^+]$ ratio). Thus, if vertical

transport is the cause of the negative trend in foE, it must be working on the ion composition or ionisable neutral composition to increase the recombination rate. In saying this, we can probably eliminate the effect of negative ions on the recombination rate: although the presence of negative ions increases recombination, this would again be expected to be a night-time effect since destruction is rapid in visible light.

We turn our attention to the production term. In the absence of direct measurements of I_∞, using sunspot number as a proxy, there is no compelling evidence for a well behaved quasi-linear trend in solar intensity, and furthermore we have endeavoured to remove such effects when arriving at foE'. The remaining contribution to q_m comes from the ionisation efficiency, C; a steadily changing neutral composition could result in a corresponding decrease in C – this must remain a purely speculative scenario though.

Considering the trends in E-region altitude now, we must try to identify a mechanism that scarcely existed during prior to 1970, but that rather abruptly began to affect the atmosphere in the 1970's. It has been suggested that changes in the geomagnetic field may be responsible for observed trends in the F2 parameters (Elias and de Adler, 2006), a mechanism in which changes in geomagnetic inclination lead to corresponding changes in vertical transport of plasma driven by the meridional flow. At Tromsø, at midday (i.e. the nominal time for all ionospheric soundings used in this study) there is a solar driven transport of plasma northward over the pole.
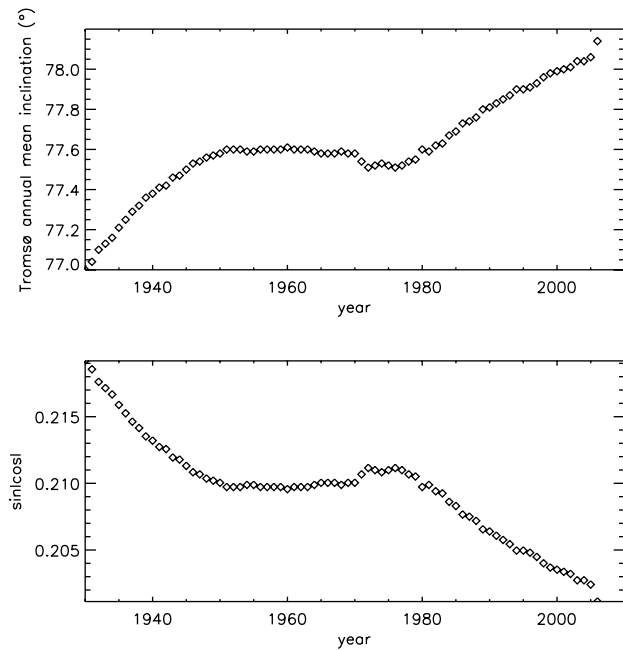
Fig. 8. Upper panel: geomagnetic inclination I at Tromsø; lower panel corresponding $\sin I \cos I$.

This meridional flow U "pushes" the plasma downwards on the day-side with a vertical component $U \sin I \cdot \cos I$ where I is the inclination of the field lines. As we see in Fig. 8, the geomagnetic inclination has indeed undergone an abrupt change in the late 1970s and we have determined the factor $\sin I \cdot \cos I$. Given a quasi constant meridional wind (i.e. with no trend), the downward forcing of the ionosphere would have been more or less constant between the late 1940s and late 1970s and thereafter decreased by approximately 5% during the subsequent period until present. At first sight this appears to explain the results. However, although the "breakpoint" in I indeed corresponds to that in $h'E'$, this mechanism would imply an increasing, rather than decreasing, $h'E'$. In any case, it is doubtful that this wind-induced drift is at all significant in the E-layer given the very strong photochemical control.

Therefore, until we are able to investigate long-term trends in upper mesosphere – lower thermosphere dynamics, the shrinking of the middle atmosphere remains a realistic candidate for the downshifting of thermospheric pressure levels and consequently the E-region.

4 Conclusions

We have identified long-term downward trends in the E-region critical frequency and altitude. The two trends, however, do not exhibit the same signature, the former being monotonic over the time scale 1935–2007, whereas the latter is not significant until the late 1970s.

We conclude that two, or possibly more mechanisms, are at work, but we are unable to arrive at unambiguous hypotheses for the causes. Scenarios such as forcing of plasma up or down magnetic field lines with varying inclination (proposed for the F-region by Elias and de Adler, 2006) to explain the downward trend in height post 1970–1980 and downward transport of NO to explain a decreasing E-region electron density are not viable for these western Europe observations (Danilov, 2001; Bremer, 1998). Solar forcing, at least as indicated by sunspot number as a proxy, can also probably be discounted.

Even though we are unable to explain them differing altitude and electron density trends are a reality.

References

Brekke, A.: Physics of the Upper Polar Atmosphere, 491 pp., Wiley-Praxis, Chichester UK, 1997.

Bremer, J.: Trends in the ionospheric E and F regions over Europe, Ann. Geophys., 16, 986–996, 1998, http://www.ann-geophys.net/16/986/1998/.

Bremer, J.: Trends in the thermosphere derived from global ionosonde observations, Adv. Space Res., 28(7), 997–1006, 2001.

Cannon, P. S., Rogers. N. C., and Hall, C. M.: Trends in Critical Frequencies and Layer Heights over Tromsø and their Consequential Impact for Radio System Modelling, Adv. Space Res., 34, 2085–2091, doi:10.1016/j.asr.2004.03.018, 2004.

Danilov, A. D.: Long-term changes of the mesosphere and lower thermosphere temperature and composition, Adv. Space Res., 20, 1265–1268, 1997.

Danilov, A. D.: Do ionospheric trends indicate to the greenhouse effect, Adv. Space Res., 28, 987–996, 2001.

Elias, A. G. and de Adler, N. O.: Earth magnetic field and geomagnetic activity effects on long-term trends in the F2 layer at mid-high latitudes, J. Atmos. Sol.-Terr. Phy., 68, 1871–1878, doi:10.1016/j.jastp.2006.02.08, 2006.

Hall, C. M. and Cannon, P. S.: Indication of the shrinking atmosphere above Tromsø (69° N, 19° E), Atmos. Phys. Lett., 80–84, doi:10.1006/asle.2001.0036, 2001.

Hall, C. M. and Cannon, P. S.: Trends in foF2 above Tromsø (69° N 19° E), Geophys. Res. Lett., 29, 2128, doi:10.1029/2002GL016259, 2002.

Hall, C. M. and Hansen, T. L.: 20th Century operation of the Tromsø Ionosonde, Adv. Polar Upper Atmos. Res., 17, 155–166, 2003.

Hall, C. M., Brekke, A., Manson, A. H., Meek, C. E., and Nozawa, S.: Trends in mesospheric turbulence at 70° N, Atmos. Sci. Lett., 8, 80–84, doi:10.1002/asl.156, 2007.

Hargreaves, J. K.: The Solar-Terrestrial Environment, 420 pp., Cambridge, UK, 1992.

Jarvis, M. J., Jenkins, B., and Rodgers, G. A.: Southern hemisphere observations of a long-term decrease in F region altitude and thermospheric wind providing possible evidence for global thermospheric cooling, J. Geophys. Res., 103, 20 744–20 787, 1998.

Qian, L., Roble, R. G., Solomon, S. C., and Kane, T. J.: Calculated and observed climate changes in the thermosphere, and a prediction for solar cycle 24, Geophys. Res. Lett., 33, L23705, doi:10.1029/2006GL027185, 2006.

Rishbeth, H.: A greenhouse effect in the ionosphere?, Planet. Space Sci., 38, 945–948, 1990.

Roble, R. G. and Dickinson, R. E.: How will changes in carbon dioxide and methane modify the mean structure of the mesosphere and thermosphere? Geophys. Res. Lett., 16, 1441–1444, 1989.

Taylor, J. R.: An Introduction to Error Analysis, 327 pp., University Science Books, California, USA, 1997.

Ulich, T. and Turunen, E.: Evidence for long-term cooling of the upper atmosphere in ionosonde data, Geophys. Res. Lett., 24, 1103–1106, 1997.